

REPORT

DEVELOPMENTAL BIOLOGY

Functional primordial germ cell-like cells from pluripotent stem cells in rats

Mami Oikawa^{1,2,†}, Hisato Kobayashi³, Makoto Sanbo², Naoaki Mizuno⁴, Kenyu Iwatsuki^{1,5}, Tomoya Takashima^{3,6}, Keiko Yamauchi², Fumika Yoshida², Takuya Yamamoto^{7,8,9}, Takashi Shinohara¹⁰, Hiromitsu Nakauchi^{4,11}, Kazuki Kurimoto³, Masumi Hirabayashi^{2,12,*}, Toshihiro Kobayashi^{1,2,*†}

The *in vitro* generation of germ cells from pluripotent stem cells (PSCs) can have a substantial effect on future reproductive medicine and animal breeding. A decade ago, *in vitro* gametogenesis was established in the mouse. However, induction of primordial germ cell-like cells (PGCLCs) to produce gametes has not been achieved in any other species. Here, we demonstrate the induction of functional PGCLCs from rat PSCs. We show that epiblast-like cells in floating aggregates form rat PGCLCs. The gonadal somatic cells support maturation and epigenetic reprogramming of the PGCLCs. When rat PGCLCs are transplanted into the seminiferous tubules of germline-less rats, functional spermatids—that is, those capable of siring viable offspring—are generated. Insights from our rat model will elucidate conserved and divergent mechanisms essential for the broad applicability of *in vitro* gametogenesis.

In mammals, primordial germ cells (PGCs), which are the precursors of sperm and eggs, emerge from the pregastrulating epiblast. Studies using genetically modified mice have uncovered key inductive signals and transcriptional regulators that are essential for PGC fate (1). However, low numbers (~40 in mice) of PGCs in early embryos offer a limited amount of material to access the specific time window when germ cells are specified. A pioneering study from 2011 reconstituted mouse germ cell specification *in vitro* by differentiating mouse pluripotent stem cells (PSCs) into PGC-like cells (PGCLCs) capable of gametogenesis *in vivo*, yielding normal offspring through assisted reproductive technology (2). Similar *in vitro* systems for other mammalian PSCs, including

humans, have revealed conserved and divergent mechanisms underlying PGC specification (3–6). Although the mouse PGCLC (mPGCLC) study was conducted a decade ago, fully functional *in vitro*-derived PGCLCs capable of producing gametes have not been reported for any other species. In this study, we demonstrate the successful generation of functional PGCLCs from PSCs in rats (*Rattus norvegicus*).

Rats and mice share important features; however, they are distinct species with substantial differences in physiology, pharmacology, cognition, and behavior (7). Although mouse embryonic stem cells (ESCs) were derived more than 40 years

ago, isolating rat germline-competent ESCs has proven to be much more challenging because of stringent culture requirements (8, 9). Hence, mice represent the preeminent rodent model system. Recently, we have made considerable progress in understanding germline development in rats using mutant strains and xenogenic models (10, 11). These advances enable us to explore rat *in vitro* gametogenesis.

After implantation, the rat blastocyst, similar to the mouse blastocyst, forms an egg-cylinder structure that contains a pluripotent epiblast from which germ cells arise (Fig. 1A). We tested whether we could use the culture conditions established for the mouse [N2B27 medium with 1% knockout serum replacement (KSR), activin, and basic fibroblast growth factor (bFGF)] to direct rat PSCs (rPSCs) toward the epiblast-like cell (EpiLC) fate for the specification of PGCs. To monitor the transition out of the pluripotent state, we used *Prdm14-H2BVenus* rat ESCs (rESCs) because *Prdm14-H2BVenus* specifically marks the naïve pluripotent epiblast and ESCs, but not the postimplantation formative or primed epiblast (10). We found that rESCs do not grow like mouse ESCs (mESCs), which grow as an adherent monolayer in EpiLC medium (fig. S1A). Instead, undifferentiated rESCs attach loosely to the feeder cells (fig. S1, B and C) (9). We reasoned that a floating aggregate culture might support survival and exit from the naïve pluripotent state in rESCs. Therefore, we seeded trypsinized rESCs into low-attachment U-bottom plates and cultured them for 72 hours in EpiLC medium. rESCs readily form aggregate-like embryoid bodies without extensive cell death (fig. S1D). By 72 hours of culture, the aggregates show reduced levels of *Prdm14-H2BVenus*, increased

¹Division of Mammalian Embryology, Center for Stem Cell Biology and Regenerative Medicine, The Institute of Medical Science, The University of Tokyo, Minato-ku, Tokyo 108-8639, Japan. ²Center for Genetic Analysis of Behavior, National Institute for Physiological Sciences, Okazaki, Aichi 444-8787, Japan. ³Department of Embryology, Nara Medical University, Kashihara, Nara 634-0813, Japan. ⁴Division of Stem Cell Therapy, Distinguished Professor Unit, The Institute of Medical Science, The University of Tokyo, Minato-ku, Tokyo 108-8639, Japan. ⁵Graduate School of Medicine, Science and Technology, Shinshu University, Ueda, Nagano 386-8567, Japan. ⁶Department of Bioscience, Tokyo University of Agriculture, Setagaya-ku, Tokyo 156-8502, Japan. ⁷Center for iPS Cell Research and Application, Kyoto University, Sakyo-ku, Kyoto 606-8507, Japan. ⁸Institute for the Advanced Study of Human Biology, Kyoto University, Sakyo-ku, Kyoto 606-8501, Japan. ⁹Medical-risk Avoidance Based on iPS Cells Team, RIKEN Center for Advanced Intelligence Project, Sakyo-ku, Kyoto 606-8507, Japan. ¹⁰Department of Molecular Genetics, Graduate School of Medicine, Kyoto University, Sakyo-ku, Kyoto 606-8501, Japan. ¹¹Institute for Stem Cell Biology and Regenerative Medicine, Department of Genetics, Stanford University School of Medicine, Stanford, CA 94305, USA. ¹²The Graduate University of Advanced Studies, Okazaki, Aichi 444-8787, Japan. *Corresponding author. Email: tkoba@g.ecc.u-tokyo.ac.jp (T.K.); mhirarin@nips.ac.jp (M.H.) †These authors contributed equally to this work.

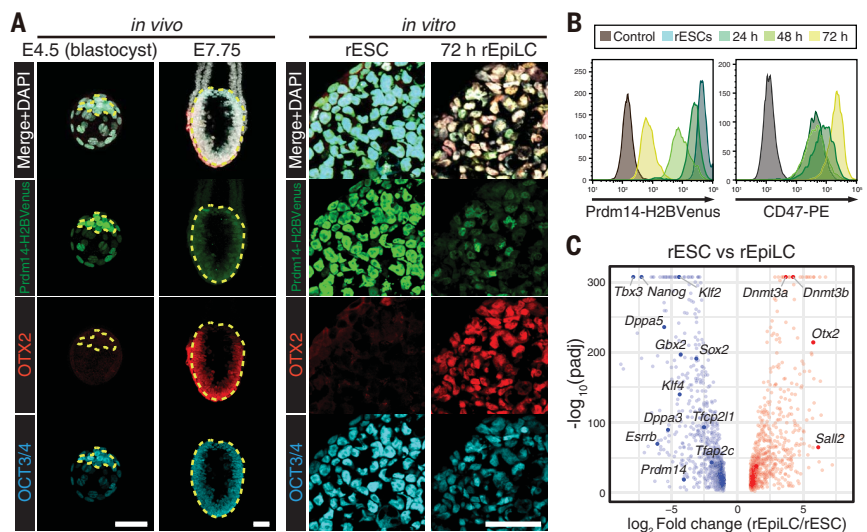


Fig. 1. Induction of rEpiLCs from rESCs. (A) IF images of rat blastocysts at E4.5 and a postimplantation embryo at E7.75 (whole mount), rESCs, and rEpiLCs (cryosection). The yellow dashed lines indicate the inner cell mass at E4.5 and the epiblast at E7.75. DAPI, 4',6-diamidino-2-phenylindole. (B) FACS patterns for *Prdm14-H2BVenus* and CD47, with nonreporter and nonstaining rESCs used as controls, respectively. (C) Volcano plot showing DEGs between rESCs and rEpiLCs. Scale bars are 50 μm . padj, adjusted *p* value.

levels of OTX2 (a postimplantation epiblast marker) and CD47 (a plasma membrane marker up-regulated in mouse epiblast stem cells) (12), and steady levels of OCT3/4 (a core pluripotency factor) (Fig. 1, A and B, and fig. S1D). Thus, our culture conditions induced key features of EpiLC fate in the rat.

To examine the global gene expression in rat EpiLCs (rEpiLCs), we performed RNA sequencing (RNA-seq) on rEpiLCs and compared them with rESCs. We identified differentially expressed genes (DEGs) among rESCs and rEpiLCs (Fig. 1C). Each group contained naïve or formative and primed associated genes (highlighted in Fig. 1C). Taken together, we conclude that rEpiLCs in spherical aggregates induced from naïve rESCs recapitulate features of the in vivo postimplantation epiblast. It is not clear as to why rPSCs do not form an adherent two-dimensional (2D) culture; however, the floating aggregates seem to physiologically resemble in vivo 3D epiblasts. Indeed, the same 3D system can also be applied to mESCs (fig. S1E).

Next, we tested whether the rEpiLCs induced from rESCs are competent for PGC fate. We isolated ex vivo epiblast from rat embryos at embryonic day 7.75 (E7.75), which is before rat PGCs (rPGCs) are specified (10), and optimized culture conditions to maintain cell viability and induce PGC fate from the epiblast (rEpiPGCs). We determined the optimal PGCLC medium composition to be that containing N2B27 medium with 5% KSR, bone morphogenetic protein-4 (BMP4), stem cell factor (SCF), leukemia inhibitory factor (LIF), and epidermal growth factor (EGF) (methods and fig. S1, F to I). To exclude potential contamination with pluripotent rESCs, which also highly express *Prdm14* (figs. S1D and S2D), we generated *Nanos3-T2A-tdTomato* reporter rats to monitor the expression of *Nanos3*, a highly conserved germ cell marker. *Nanos3-T2A-tdTomato* is specifically expressed in E9.5 to E15.5 rPGCs, rEpiPGCs, and spermatogonia in the adult testes, but not in pre- and postimplantation epiblasts (fig. S2, A to I). rESCs derived from *Nanos3-T2A-tdTomato* reporter rats (N3T-rESCs) did not show expression of tdTomato in an undifferentiated state (fig. S2D). We also confirmed that N3T-rESCs efficiently contribute to the germline in vivo after injection into blastocysts (fig. S2, J and K). Therefore, we used N3T-rESCs for the induction of rEpiLCs and subsequent rat PGCLCs (rPGCLCs).

Dissociated rESCs were cultured for 48 to 72 hours in EpiLC medium to form aggregates, which were transferred into PGCLC medium containing BMP4, a cytokine that is critical for PGC fate (13) (Fig. 2A). Within 2 days of culture in the PGCLC medium, a proportion of cells in the aggregates started to show expression of *Nanos3-T2A-tdTomato* in response to BMP4 (Fig. 2B and fig. S3, A to E). The expression peaked at days 2 and 3 and then gradually declined by day 5, likely owing to low prolif-

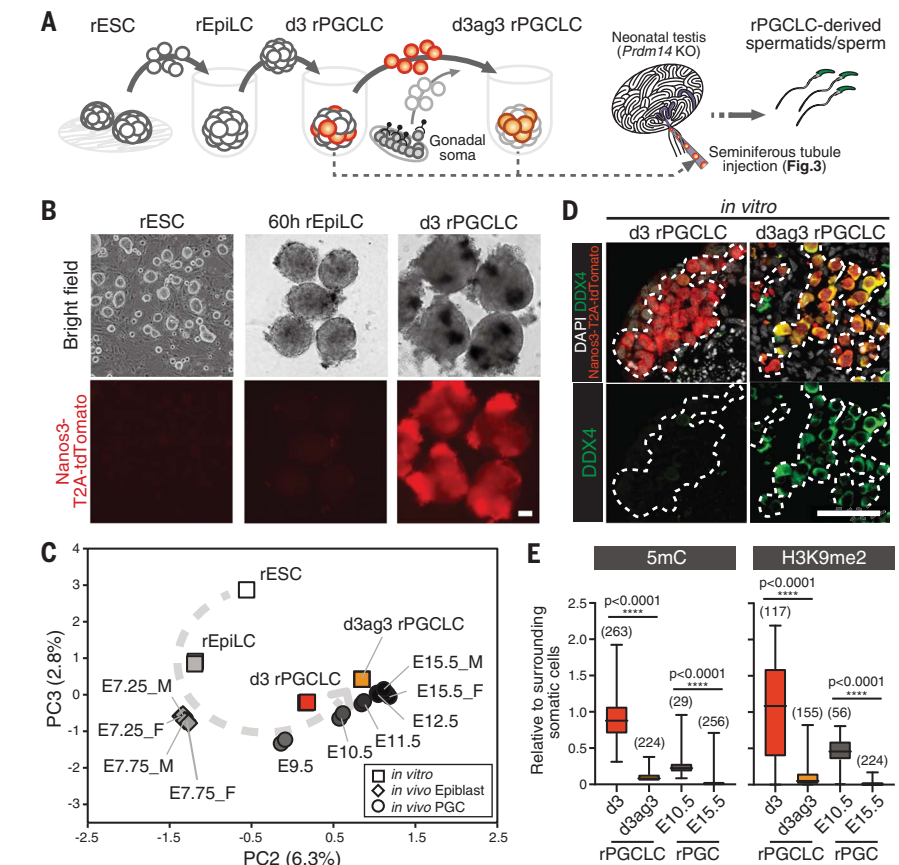


Fig. 2. Induction and maturation of rPGCLCs from rEpiLCs. (A) Experimental design for rPGCLC induction. (B) Morphology of aggregates during rPGCLC induction from N3T-rESCs visualized by bright-field (top) and fluorescence imaging (bottom). (C) PCA to compare in vitro and in vivo samples. The gray dashed line represents a trajectory of germline development. (D) IF images of a cryosection showing DDX4 expression during rPGCLC maturation in vitro. The white dashed lines indicate N3T⁺ rPGCLCs. (E) Quantification of the indicated epigenetic marks. The averages and SD are shown. Numbers in parentheses indicate the number of rPGCs or rPGCLCs counted from IF images. Significance was determined using the Mann-Whitney test. 5mC, 5-methylcytosine; H3K9me2, dimethylated histone 3 lysine 9. Scale bars are 100 μ m in (B) and 50 μ m in (D).

erative activity of nascent rPGCLCs, as in mice (fig. S3C) (2). We used Immunofluorescence (IF) staining to confirm that N3T⁺ cells coexpress the PGC and pluripotency markers *Tfap2c*, *Oct3/4*, and *Sox2*, indicating that they resemble in vivo rPGCs (fig. S3, F and G). rEpiLCs cultured for 48 to 60 hours showed the highest numbers of rPGCLCs (fig. S3H). This time is longer than that for PGCLC induction in mice, which peak around 36 to 48 hours (2, 14). The time lag may be attributed to the 1.5- to 2-day difference in gestation period for the mouse versus rat (10, 15).

We next analyzed the transcriptome of day 3 (d3) rPGCLCs by RNA-seq and compared it with the transcriptomes of rESCs, rEpiLCs, in vivo rat epiblast, and rPGCs (10). Hierarchical clustering and correlation coefficient evaluation of the samples showed that d3 rPGCLCs closely correlated with E9.5 to E11.5 early rPGCs (fig. S4, A and B). In the principal components analysis (PCA), the PC2-PC3 plot reflects the progression of epiblast toward germline fate both in vivo and in vitro (Fig. 2C). The d3 rPGCLCs

expressed all the PGC specifiers and pluripotency genes, whereas late PGC marker expression is lower than that in E15.5 gonadal rPGCs (fig. S4, C and D). Taken together, we conclude that the induced rPGCLCs might be equivalent to the migratory stage of in vivo rPGCs.

To investigate the potential of rPGCLCs to mature into late PGCs, we reconstituted a gonadal environment using rPGCLCs and gonadal somatic cells, as described for mice (14) (Fig. 2A). We used E15.5 rat gonads because their sex can be clearly distinguished morphologically. To eliminate endogenous rPGCs in gonads, we explored rPGC-specific cell surface markers. Notably, stage-specific embryonic antigen 1 (SSEA1), a widely used surface marker for mouse PGCs (mPGCs), is not expressed in rPGCs (fig. S5A). From our transcriptome dataset, we found that *c-Kit* is highly up-regulated in both in vitro and in vivo rPGCs (fig. S4D). The expression of *c-KIT* overlaps with *Prdm14* and *Nanos3* reporters in d3 rPGCLCs and E15.5 gonadal rPGCs (fig. S5, B to E). Day 3 male N3T⁺

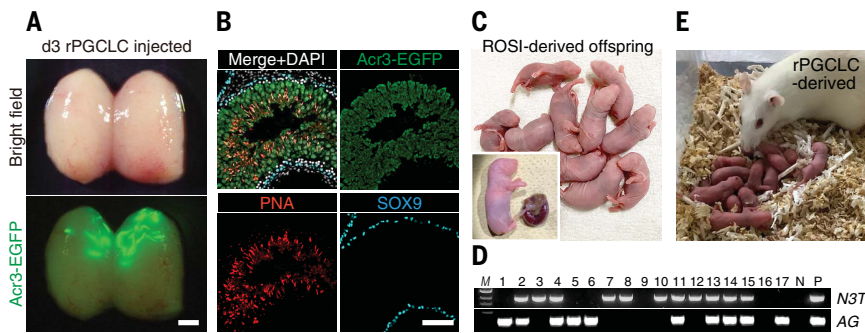


Fig. 3. Functional validation of rPGCLCs. (A) *Prdm14* KO rat testis at 10 weeks after transplantation of day 3 male N3T/AG-rPGCLCs, visualized by bright-field (top) and fluorescence imaging (bottom). (B) IF of a cryosection showing testis 10 weeks after transplantation of N3T/AG-rPGCLCs. (C) Offspring from rPGCLC-derived spermatids generated by ROSI. The inset shows an offspring with placenta. (D) Representative genotyping result of rPGCLC-derived offspring. M, molecular marker; 1 to 17, samples obtained from individual rPGCLC-derived offspring; N, negative control (water); P, positive control (N3T/AG-rESCs). (E) Female rat derived from N3T/AG-rPGCLCs and its offspring. Scale bars are 2 mm in (A) and 100 μ m in (B).

Table 1. Spermatogenesis efficiency after rPGCLC transplantation.

rPGC or rPGCLC stage	Parental cells	Number of testes transplanted	Number of testes with successful transfer	Number of testes with EGFP-positive tubules	Number of EGFP-positive tubules in each testis
d3 rPGCLC	N3T/AG-rESCs no. 3	13	9 of 13 (69%)	6 of 9 (67%)	>5, >5, 4, 4, 1, 1
d3 rPGCLC	N3T/AG-rESCs no. 2	12	7 of 12 (58%)	6 of 7 (86%)	>5, >5, >5, >5, 4, 3
d4 rPGCLC	N3T/AG-rESCs no. 11	4	4 of 4 (100%)	2 of 4 (50%)	>5, 2
d3ag3 rPGCLC	N3T/AG-rESCs no. 3	2	1 of 2 (50%)	1 of 1 (100%)	>5
d3ag3 rPGCLC	N3T/AG-rESCs no. 2	2	1 of 2 (50%)	1 of 1 (100%)	>5
In vivo rPGC	N3T/AG E15.5 male gonad	4	2 of 4 (50%)	2 of 2 (100%)	>5, >5

rPGCLCs were aggregated with c-KIT⁺ rPGC-depleted male or female gonadal somatic cells from wild-type rats and cultured for 3 to 6 days (ag3 to ag6; fig. S6A). Male rPGCLCs that aggregated with male gonadal somatic cells lost *Nanos3-T2A-tdTomato* expression by day 3 (fig. S6, A and B), indicating the need for further optimization, as has recently been demonstrated for organ culture of neonatal rat testes (16). By contrast, female gonadal somatic cells could support the survival of male N3T⁺ rPGCLCs (fig. S6, A and B). d3ag3 rPGCLCs show an up-regulation of the markers for late PGCs and some meiosis-related genes, unlike d3 rPGCLCs (Fig. 2D and figs. S4, C and D, and S6C). Notably, the transcriptome of d3ag3 rPGCLCs is similar to that of E12.5 to E15.5 late rPGCs, and the PCA showed a comparable trajectory to germline development in vivo (Fig. 2C and fig. S4, A and B). Because PGCs undergo extensive epigenetic reprogramming during development, we next examined DNA methylation and histone methylation dynamics in culture. The dynamics of the

epigenetic changes in culture closely correlate with in vivo rPGC development (Fig. 2E and fig. S6, D and E), suggesting that d3 rPGCLCs mature in vitro toward the gonadal stage with stepwise progression of epigenetic reprogramming.

Finally, we investigated whether the male rPGCLCs undergo spermatogenesis in vivo after transplantation into testes (Fig. 2A). To monitor germ cell progression in the recipient testes, we generated *Acr3-EGFP* (AG) transgenic rats that show expression of enhanced green fluorescent protein (EGFP) specifically in spermatocytes, round spermatids, and mature sperm in the testis under the control of the *Acrosin* promoter (fig. S7, A to E). We derived rESCs from blastocysts obtained by crossing a *Nanos3-T2A-tdTomato* rat with an *Acr3-EGFP* rat (hereafter, N3T/AG-rESCs). N3T⁺ day 3 to 4 (d3-4) rPGCLCs or d3ag3 rPGCLCs sorted by fluorescence-activated cell sorting (FACS) were transplanted into the seminiferous tubules of *Prdm14* knockout (*Prdm14* KO) neonatal rats that completely lacked endogenous germ cells

(11) (fig. S8A). Eight to 11 weeks after transplantation, we detected *Acr3-EGFP* expression in the seminiferous tubules in both d3-4 and d3ag3 rPGCLC transplanted testes (Table 1, Fig. 3A, and fig. S8, B, C, and E). The testicular spermatozoon showed EGFP in the nucleus (fig. S8D). In the sections, we observed peanut agglutinin (PNA)-positive round spermatids and mature sperm (Fig. 3B), demonstrating that rPGCLCs can complete spermatogenesis in vivo.

The spermatogenic capacity of rPGCs and rPGCLCs is comparable to that of mPGCs and mPGCLCs (2) but lower than mouse spermatogonial and germline stem cells, likely because of their developmental differences (17, 18). Obtaining rPSC-derived offspring through natural mating may require further maturation of rPGCLCs into these stem cells; this merits additional investigation for future animal-breeding applications. Instead, we confirmed the developmental potential of rPGCLC-derived testicular germ cells by injecting round spermatid and testicular sperm into the oocytes obtained from wild-type rats using round spermatid injection (ROSI) and testicular sperm extraction with intracytoplasmic sperm injection (TESE-ICSI), respectively. At full term after embryo transfer, 18 (ROSI) and 6 (TESE-ICSI) live offspring were born and appeared healthy (Fig. 3C, fig. S8F, and table S3). Both *N3T* and *AG* transgenes originating from rESCs were successfully transmitted to the offspring (Fig. 3D). Whereas the body weights of the offspring were in the normal range, the placenta that was derived from ROSI offspring was significantly larger than that from control rats (fig. S8, G to I). Nevertheless, the offspring developed into fertile and normal adults (Fig. 3E and fig. S8J), suggesting that the induced rPGCLCs in vitro are functional and capable of producing mature gametes.

In vitro systems that differentiate rPSCs to rPGCLCs could become a useful platform to examine the function of key transcriptional regulators during the transition of naïve-to-formative pluripotency and during PGC specification. As exemplified by PSC research (19), insights from rats, a distinctive alternative model to the mouse, will help to define conserved or divergent principles in germ cell development within rodents and across mammals. In primates, PGCLCs can mature to the gonadal stage in vitro or in vivo (20, 21) but do not progress to the gamete stage, perhaps owing to limitations in culture conditions or the lack of suitable models to test their function in vivo. However, rodents provide an excellent system for readily testing the fertility and developmental potential of in vitro germ cells. Because rats are physiologically more similar to humans than mice (7), our in vitro gametogenesis system offers the opportunity to screen causative factors in inter- or transgenerationally inherited disorders. Advances in the rat model should take us a step closer to achieving applicable systems

for other species in domestic animal breeding and reproductive medicine.

REFERENCES AND NOTES

1. M. Saitou, M. Yamaji, *Cold Spring Harb. Perspect. Biol.* **4**, a008375 (2012).
2. K. Hayashi, H. Ohta, K. Kurimoto, S. Aramaki, M. Saitou, *Cell* **146**, 519–532 (2011).
3. N. Irie *et al.*, *Cell* **160**, 253–268 (2015).
4. T. Kobayashi *et al.*, *Nature* **546**, 416–420 (2017).
5. T. Kobayashi *et al.*, *Cell Rep.* **37**, 109812 (2021).
6. K. Sasaki *et al.*, *Cell Stem Cell* **17**, 178–194 (2015).
7. T. J. Aitman *et al.*, *Nat. Genet.* **40**, 516–522 (2008).
8. M. Buehr *et al.*, *Cell* **135**, 1287–1298 (2008).
9. P. Li *et al.*, *Cell* **135**, 1299–1310 (2008).
10. T. Kobayashi *et al.*, *Development* **147**, dev.183798 (2020).
11. T. Kobayashi *et al.*, *Nat. Commun.* **12**, 1328 (2021).
12. P. J. Rugg-Gunn *et al.*, *Dev. Cell* **22**, 887–901 (2012).
13. Y. Ohinata *et al.*, *Cell* **137**, 571–584 (2009).
14. K. Hayashi *et al.*, *Science* **338**, 971–975 (2012).
15. M. A. Hill, Embryology—Main page; https://embryology.med.unsw.edu.au/embryology/index.php/Main_Page.
16. T. Matsumura *et al.*, *Sci. Rep.* **11**, 3458 (2021).
17. H. Ohta, T. Wakayama, Y. Nishimune, *Biol. Reprod.* **70**, 1286–1291 (2004).
18. Y. Ishikura *et al.*, *Cell Rep.* **17**, 2789–2804 (2016).
19. Q. L. Ying, A. Smith, *Stem Cell Reports* **8**, 1457–1464 (2017).
20. E. Sosa *et al.*, *Nat. Commun.* **9**, 5339 (2018).
21. C. Yamashiro *et al.*, *Science* **362**, 356–360 (2018).

ACKNOWLEDGMENTS

We thank members of the Hirabayashi lab, in particular, M. Hashimoto and N. Niizeki for help with animals and M. Ohnishi for secretarial support. We also thank R. Sengupta for editing and providing critical input to the manuscript. We thank T. Hayama for his advice on the reaggregation of rat gonads. We thank S. Matoba for his advice on the culture of reconstructed gonads and histological analysis of placentas. We thank the Spectrography and Bioimaging Facility, National Institute for Basic Biology (NIBB) Core Research Facilities, for technical support. Flow cytometry was performed in the National Institute for Physiological Sciences (NIPS), Sciences–Exploratory Research Center on Life and Living Systems (ExCELLS); and in The Institute of Medical Science, The University of Tokyo (IMSUT) FACS Core laboratory. We also thank the Pathology Core Laboratory in IMSUT for technical support and the Single-Cell Genome Information Analysis Core (SignAC) in the Institute for the Advanced Study of Human Biology (ASHBi) for RNA sequence analysis. **Funding:** This work was supported by Grants-in-Aid for Scientific Research (KAKENHI) from the Japan Society for the Promotion of Science grants 18H02367 to M.H. and T.K., 18H05548 to T.K., 18H05544 to T.K. and K.K., 19K23711 to M.O., and 21H02382 to H.K.; Japan Agency for Medical Research and Development (AMED) grants JP18gm0010002 to H.N. and M.H. and JP18bm0704022 to T.K.; The Sumitomo Foundation grant 210348 to T.K.; and a NIPS research grant for young scientists to M.O. This work was also supported by grants from the Cooperative Study Program (21-147) of NIPS and the Cooperative Research Grant of the Genome Research for BioResource, NODAI

Genome Research Center, Tokyo University of Agriculture. **Author contributions:** M.O. and T.K. designed the experiments. M.O., H.K., M.S., K.I., K.Y., F.Y., M.H., and T.K. performed the experiments. H.K., T.T., T.Y., and K.K. contributed to the RNA-seq analyses. N.M., T.S., and H.N. contributed resources. M.O., H.K., K.K., and T.K. analyzed and interpreted the data. M.O. and T.K. wrote the manuscript. **Competing interests:** The authors declare no competing interests. **Data and materials availability:** RNA-seq data have been deposited in the Gene Expression Omnibus (GEO) under accession number GSE178701. Rat strains *Nanos3-T2A-tdTomato* (knock-in reporter rat) and *Acr3-EGFP* (transgenic reporter rat) and cell lines N3T-rESC and N3T/AG-rESC are available from T. Kobayashi and M. Hirabayashi under a material transfer agreement with The University of Tokyo or NIPS.

SUPPLEMENTARY MATERIALS

science.org/doi/10.1126/science.abl4412

Methods

Figs. S1 to S8

Tables S1 to S3

References (22–35)

MDAR Reproducibility Checklist

[View/request a protocol for this paper from Bio-protocol.](#)

13 July 2021; accepted 4 March 2022

10.1126/science.abl4412

Functional primordial germ cell–like cells from pluripotent stem cells in rats

Mami OikawaHisato KobayashiMakoto SanboNaoaki MizunoKenyu IwatsukiTomoya TakashimaKeiko YamauchiFumika YoshidaTakuya YamamotoTakashi ShinoharaHiromitsu NakauchiKazuki KurimotoMasumi HirabayashiToshihiro Kobayashi

Science, 376 (6589), • DOI: 10.1126/science.abl4412

Generating functional rate gametes

In the past decade, methods have been developed to generate germ cells from pluripotent stem cells for studies of development and in vitro gametogenesis. However, offspring from in vitro–derived germ cells has only been achieved in mice. Oikawa *et al.* extend this work beyond mice to a second rodent species, the rat, a leading animal model for biomedical research with many physiological similarities to humans. A stepwise protocol allows for the production of fetal stage rat germ cells that can produce viable offspring upon maturation in the testis and injection of the sperm into unfertilized oocytes. This system will allow comparative studies and enable broader execution and analysis of in vitro gametogenesis. —BAP

View the article online

<https://www.science.org/doi/10.1126/science.abl4412>

Permissions

<https://www.science.org/help/reprints-and-permissions>

Use of this article is subject to the [Terms of service](#)

Science (ISSN) is published by the American Association for the Advancement of Science. 1200 New York Avenue NW, Washington, DC 20005. The title *Science* is a registered trademark of AAAS.

Copyright © 2022 The Authors, some rights reserved; exclusive licensee American Association for the Advancement of Science. No claim to original U.S. Government Works